## Biosynthesis of an Opine Metallophore by *Pseudomonas aeruginosa*

Jeffrey S. McFarlane and Audrey L. Lamb*

### Supporting Information

### Supplementary Methods

#### Protein Expression and Purification

Gene sequences for the *P. aeruginosa* PAO1 strain nicotianamine synthase (NAS) (PA4836) and opine dehydrogenase (ODH) (PA4835) were acquired from the *Pseudomonas* Genome Database[1]. Sequences for *S. aureus* were acquired from the methicillin-resistant Mu50 strain with NCBI accession numbers WP_001058848.1 (NAS) and WP_000040588.1 (ODH). These sequences were codon optimized for expression in *E. coli* by GenScript. The *P. aeruginosa* sequences were ligated into pET28b vectors and the *S. aureus* sequences were ligated into pET15TV vectors, both with N-terminal hexahistidine tags. The plasmids were transformed into New England Biolabs BL21 (DE3) cells for expression.

Following growth of a 50 mL overnight culture at 37 °C, baffled flasks with 1L of LB media containing 50 mg/mL kanamycin (pET28b) or 200 mg/mL ampicillin (pET15TEV) were inoculated with 10 mL of overnight culture and grown to an O.D. of 0.6 at 37 °C. Cultures were induced with 200 µL of 1 M IPTG and grown overnight at their optimal expression temperature (25 °C for PaNAS, PaODH and SaODH and 15 °C for SaNAS). After 20 hours, cells were pelleted at 4225 x g for 10 minutes. The resulting pellet was resuspended in buffer A containing 50 mM potassium phosphate pH 8, 300 mM NaCl, 50 mM imidazole and 10% glycerol. Cells were French pressed 3 times and the lysate was centrifuged 1 hour at 23,426 x g. The lysate was loaded onto a GE Healthcare nickel-chelating fast flow sepharose column. NAS proteins were eluted using a linear gradient of increasing imidazole concentration up to 500 mM. Both NAS proteins elute with a peak at approximately 275 mM. The ODHs were purified using a step gradient of 500 mM imidazole, with steps of 20% to wash out contaminating protein and 55% to elute ODH. Eluted samples were loaded directly onto a GE Superdex 200 size exclusion chromatography column pre-equilibrated with 50 mM potassium phosphate pH 8, 150 mM sodium citrate and 20% glycerol for PaNAS, PaODH and SaODH. For SaNAS, 50 mM potassium phosphate pH 8, 100 mM sodium chloride and 10% glycerol was used as the size exclusion chromatography buffer. Following purification, protein was concentrated using Millipore Amicon centrifugation concentrators with 10,000 MWCO (NAS) or 30,000 MWCO (ODH), to final concentrations of 10-12 mg/mL. These preparations yield 20 mg (PaODH), 80 mg (SaODH), 100 mg (PaNAS) and 150 mg (SaNAS) per liter of culture. Purity of each protein was evaluated using 15% Tris-HCl SDS-PAGE (**Fig. S1**). All were condsidered to be greater than 95% pure.

#### *P. aeruginosa* NAS binding affinity for SAM

To determine the binding affinity of PaNAS for *S*-adenosyl-L-methionine (SAM), a Cary Eclipse fluorometer was set to an excitation wavelength of 280 nm and an emission wavelength of 380 nm with excitation and emission slits set to 20 nm. 100 nM PaNAS in 50 mM potassium phosphate pH 8 was added to a quartz fluorometry cuvette to give a total volume of 100 µL. Increasing concentrations of SAM were titrated from 0 - 25 µM after correcting for dilution. Each concentration was measured three times per experiment and each experiment was repeated three times.

Raw data showed a decrease in fluorescence of 50 AU while titrating from 0 to 15 µM SAM. Fluorescence intensities were corrected for the inner filter effect due to SAM absorbance at 280 nm using the equation[2]:

$$Fc = F \times 10^{\frac{\varepsilon Cl}{2}}$$

where F is the measured fluorescence intensity, ε is the extinction coefficient of SAM measured at 280 nm and calculated using Beer's law, C is the concentration of SAM in M and *l* is the cuvette path length in $cm^{-1}$. The Stern-Volmer equation:

$$\frac{Fo}{Fc} = 1 + K_D[Q]$$

was initially used for $K_D$ determination due to the observed red shifted emission spectrum for PaNAS, however a graph of Fo/F vs. [SAM] produced a line with downward curvature suggesting a difference in quenching between the two tryptophans in the protein[3]. The modified Stern-Volmer equation

$$\frac{Fo}{Fo-Fc} = \frac{1}{(f_a K_Q[Q])} + \frac{1}{f_a}$$

was then used to correct for this effect[2, 3]. $f_a$ is the fractional number of fluorophores accessible to the quencher and [Q] is the concentration of quencher. Fo/(Fo-Fc) vs. 1/[Q] gave a straight line plot where the slope = $1/K_Q = K_D$ and the y-intercept = $f_a$ (**Fig. S2A**).

The change in fluorescence intensity was also plotted vs. [SAM]. The resulting curve was fit using the equation:

$$\frac{-\Delta Fc}{F} = \frac{[SAM]}{[SAM] + K_D}$$

where F is the maximal fluorescence change upon binding and $K_D$ is the dissociation constant for SAM (**Fig. S2B**).

***P. aeruginosa* ODH binding affinity for NADPH**

To determine the binding affinity of NADPH for PaODH, a Cary Eclipse fluorometer was set to an excitation wavelength of 340 nm and an emission wavelength of 450 nm with excitation and emission slits set to 10 nm. NADPH in 50 mM potassium phosphate pH 8 was added to a quartz fluorometry cuvette to yield 100 µL of total volume with an NADPH concentration of 250 nM. PaODH was titrated in increasing concentrations from 0.2 - 25 µM after correction for dilution. Each concentration was measured three times for each experiment and each experiment was repeated three times. To correct for the inner filter effect caused by increasing concentrations of protein, the fluorescence for each PaODH concentration was measured in the absence of NADPH. A plot of the change in fluorescence vs. enzyme concentration fit to a straight line which was subtracted from the titrations with NADPH present. The resulting fluorescence values were fit to the equation below (**Fig. S2C**):

$$\Delta F = \frac{F \times [NADPH]}{[NADPH] + K_D}$$

**Reconstitution of biosynthetic pathway (plate-reader assay)**

To assay different combinations of potential amino acid and α-ketoacid substrates, an assay combining both biosynthetic enzymes was developed that monitored the oxidation of NADPH to $NADP^+$ by ODH as a loss of absorbance at 340 nm. Experiments were performed using a Cary Eclipse spectrophotometer paired with a Cary 50MPR microplate reader using Costar 96 well flat-bottomed plates. Immediately prior to each experiment, a master mix of 2 µM NAS, 2 µM ODH, 200 µM SAM and 75 µM NADPH in 50 mM Tris pH 8 (*S. aureus*) or 50 mM potassium phosphate pH 8 (*P. aeruginosa*) was made. This master mix also contained 200 µM of either pyruvate, oxalaoacetate or 2-ketoglutarate. The master mix was dispensed into each of 24 wells and rocked gently for 30 seconds to mix. 2 µL of test amino acid solution was added to independent wells to a final concentration of 200 µM to initiate the reaction. Each amino acid was tested in triplicate wells. Absorbance readings at 340 nm were

immediately initiated and recorded for 20 minutes at room temperature. To determine the rate of conversion of NADPH to $NADP^+$, a standard curve was generated for the absorbance by NADPH in the 96 well plate. This resulted in a linear plot. The equation calculated from the linear fit was used to convert absorbance values to NADPH concentrations. The 42 amino acids tested are shown in **Table S1.** To determine the specificity of SaODH for pyruvate, oxaloacetate or α-ketoglutarate the assay above was repeated with 2 µM SaNAS, 2 µM SaODH, 500 µM SAM, 75 µM NADPH, 2 mM α-ketoacid and 2 mM D-histidine in 50 mM Tris pH 8. These experiments were repeated three times on separate days. These conditions were also used to compare ketoacid substrate specificity for PaODH as shown in (**Figure 4**). Oxaloacetate is known to decompose to pyruvate over time[4]. To prevent this process from contributing to the reaction rate for the *S. aureus* enzymes, oxaloacetate was solubilized immediately prior to its addition to the reaction mixture. To confirm that pyruvate was not present in the oxaloacetate solution, we performed $^{13}$C-NMR on a pyruvate standard and on an oxaloacetate sample. The resulting NMR spectrum showed no evidence of contaminating pyruvate in the oxaloacetate samples brought into solution and scanned for 20 minutes.

**Progress curves to determine amino acid selectivity**

To measure full progress curves, NADPH oxidation at 340 nm was recorded at 22 °C for 1 hour using a TgK stopped flow spectrometer with a xenon lamp. Final reaction concentrations following 1:1 mixing of syringe one and two, were 2 µM NAS, 20 µM ODH, 400 µM SAM, 400 µM α-ketoacid (PaODH - α-ketoglutarate, SaODH - pyruvate), 200 µM NADPH and 25 µM or 12.5 µM histidine (PaODH - L-histidine, SaODH - D-histidine) combined in 50 mM pH 8 buffer (Pa - $KP_i$, Sa - Tris). Syringe 1 contained the above components except for histidine. Syringe 2 contained histidine in 50 mM pH 8 buffer (Pa - $KP_i$, Sa - Tris). Each reaction was performed twice and the resulting curves averaged.

**Initial rate reactions to determine steady state kinetic parameters**

NADPH oxidation at 340 nm was recorded at 22 °C using a TgK stopped flow spectrometer with a xenon lamp. Syringe one contained 2 µM NAS, 20 µM ODH, 1200 µM SAM, 400 µM NADPH, and 2000 µM pyruvate in 50 mM pH 8 buffer (Pa - $KP_i$, Sa - Tris). The non-rate-limiting concentration of all susbtrates was determined by comparing full progress curves as described above for varied concentrations of substrates and ODH enzyme. Syringe two contained L-histidine (PaNAS) or D-histidine (SaNAS) at decreasing concentrations following a two-fold serial dilution of histidine from a starting concentration of 800 µM down to 0.78 µM in the same buffer used in syringe one. The two syringes were mixed 1:1 and initial rates were recorded for 60 seconds and the concentration series was measured four times for each enzyme. Secondary plots of initial rates were fit as described below (**Figure S4A and B**).

The secondary plot of PaNAS was fit to the quadratic form of the velocity equation[5] to account for the high concentration of enzyme (1 µM) relative to the $K_m$ (5.4 µM):

$$V_o = V_{max} \frac{([E_T]+[S_T]+[K_m]) - \sqrt{([E_T]+[S_T]+[K_m])^2 - 4[E_T][S_T]}}{2[E_T]}$$

The secondary plot of the SaNAS reaction with D-histidine was fit using the Michaelis-Menton equation:

$$V_o = \frac{V_{max}[S]}{K_m + [S]}$$

**Mass spectrometry verification of pseudopaline and staphylopine production**

Pseudopaline was produced by combining 10 µM PaNAS, 10 µM PaODH, 5 mM NADPH, 5 mM SAM, 5 mM L-histidine, and 5 mM α-ketoglutarate in 50 mM potassium phosphate pH 8. The total reaction volume was 1.5 mL and was incubated at room temperature for 2 hours while slowly rocking. After 2 hours the reaction was quenched and the protein precipitated by adding glacial acetic acid to a final concentration of 300 µM. Precipitated protein was pelleted by centrifugation for 10 min at 20,800 x g. The supernatant was removed and submitted for ESI-MS analysis. An Agilent quadrupole G6120A

coupled to an Agilent 1200 HPLC using a Waters T3 C-18 column were used for sample separation and analysis. We predicted a mass for pseudopaline following acid quench of 386.1438 ($[M+H]^+$ of 387.1438). A product *m/z* of 387.15 was detected in positive mode from the first elution peak of the solvent front using a mobile phase of 99% Water (0.05% Formic Acid): 1% MeOH (**Fig. S5A-B**). This elution peak was also found to contain L-histidine (*m/z* 156.08) (**Fig. S5B**). A high resolution mass spectrum (HRMS) was performed on a Waters LCT Premiere (Micromass, Ltd., Manchester UK) time of flight mass spectrometer with an electrospray ion source and determined to be *m/z* 387.1526 consistent with $[M+H]^+$ for pseudopaline (**Fig. S5C**). We predicted a mass for the NAS reaction product of *m/z* $[M+H]^+$ 258.12. At 1.51 min, a peak eluted with an *m/z* of 258.04 which we assume to be a small quantity of unconsumed NAS reaction product (**Fig. S5D**). We also performed a direct ESI-MS injection of supernatant from a separate reaction performed as described above. These samples were diluted 100-fold with LC-MS grade water (Sigma-Aldrich), and 10uL of each dilution was analyzed by flow injection over 2 minutes on an LCMS-IT-TOF (Shimadzu Scientific Instruments). Solvent conditions for injection were 60% of an aqueous 0.2% formic acid solution and 40% acetonitrile (Sigma Aldrich), with a total flow rate of 0.3 mL/min. An ESI source was used, and acquisition was performed in scan mode from 100-750 m/z for both positive- and negative ion modes. A 10 msec ion accumulation time was used, and event time was set to 100 msec. Using this technique, we again identified an *m/z* of 387.149 corresponding to the presence of pseudopaline (**Fig. S5E**). Staphylopine was produced by combining 10 µM SaNAS, 10 µM SaODH, 5 mM NADPH, 5 mM SAM, 5 mM D-histidine, and 5 mM pyruvate in 50 mM potassium phosphate pH 8. Following a two hour incubation at room temperature, supernatants were prepared and mass spectrometry analysis was performed as described above for pseudopaline. A product *m/z* of 329.1441 was detected in positive mode from the first elution peak (0.33 min) of the solvent front using a mobile phase of 99% Water (0.05% Formic Acid): 1% MeOH (**Fig. S6A-B**). Staphylopine was also detected following direct injection of supernatants with an *m/z* of 329.143 (**Fig. S6C**). These values correspond to the expected mass for staphylopine as first reported by Ghssein et al[6].

**Supplementary Figures**

**Figure S1. SDS PAGE analysis of purified proteins.** Lanes: *P. aeruginosa* NAS and ODH and *S. aureus* NAS and ODH. The ladder is a GOLDBIO BLUEstain protein ladder and the gel is 15% Tris-HCl.

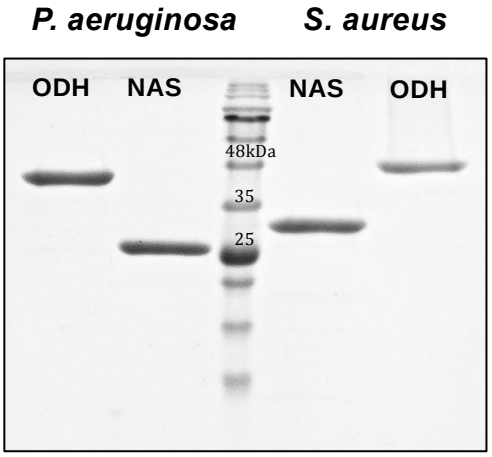

**Figure S2. Binding isotherms.** Error is the standard deviation of three trials. **A)** Stern-Volmer plot for the affinity of *P. aeruginosa* nicotianamine synthase for *S*-adenosyl-L-methionine (SAM). The resulting $K_D$ is 2.9 ± 1.1 µM. **B)** Fitted plot of decreasing PaNAS fluorescence vs. [SAM]. The resulting $K_D$ is 1.2 ± 0.3 µM. **C)** Affinity of *P. aeruginosa* opine dehydrogenase for NADPH . The NADPH was excited at 340 nm and emission was measured at 450 nm. The resulting $K_D$ was 11 ± 1 µM.

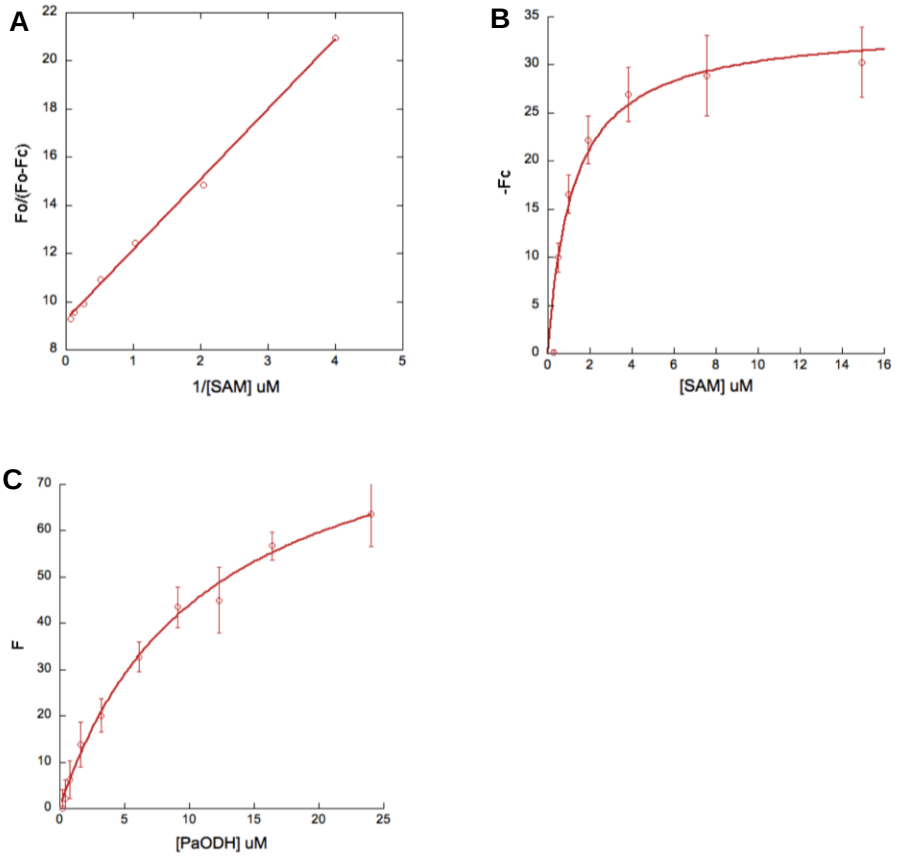


**Figure S3. Reconstitution of biosynthetic pathways to determine amino acid specificity.** Each error bar represents the standard deviation of three trials. Rates were determined using an NADPH standard curve and calculated in $\mu mol \cdot L^{-1} \cdot min^{-1}$. The non-standard abbreviations are as follows: Orn - ornithine, Nle - norleucine, Nva - norvaline, Dab - 2,4-diaminobutyric acid, Hyp - hydroxyproline **A)** *S. aureus* activity in the presence of pyruvate with varied amino acids. **B)** *P. aeruginosa* activity in the presence of pyruvate with varied amino acids. **C)** *P. aeruginosa* activity in the presence of oxaloacetate with varied amino acids. **D)** *P. aeruginosa* activity in the presence of 2-ketoglutarate with varied amino acids. Standard deviation was low for both the Sa reactions with D-histidine and the Pa reaction with L-histidine, but high for other amino acids leading us to use stopped flow spectrometry to verify catalysis for L-threonine, L-asparagine and L-hydroxyproline.

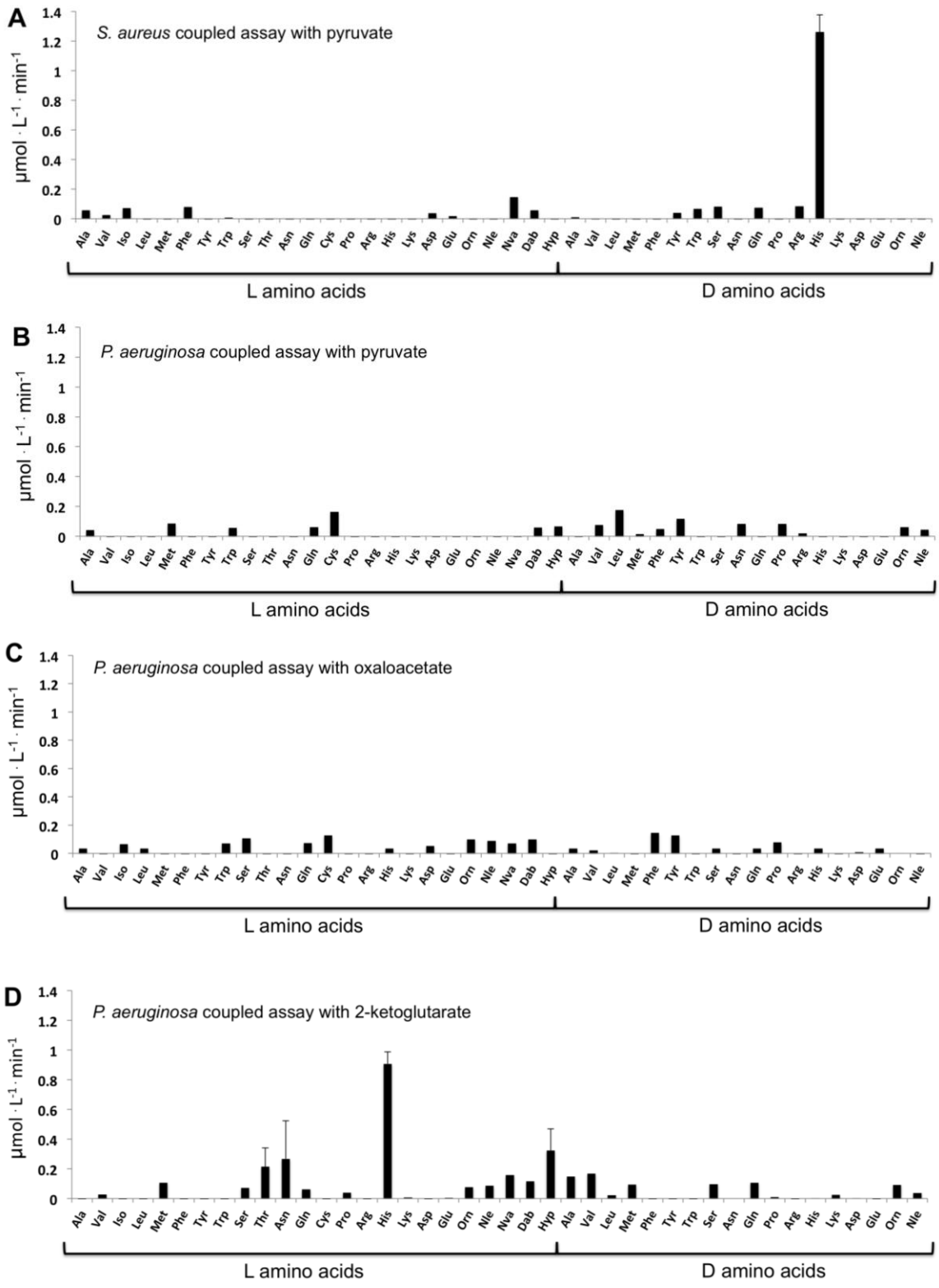
A
S. aureus coupled assay with pyruvate
B
P. aeruginosa coupled assay with pyruvate
C
P. aeruginosa coupled assay with oxaloacetate
D
P. aeruginosa coupled assay with 2-ketoglutarate
µmol · L-1 · min-1
0
0.2
0.4
0.6
0.8
1
1.2
1.4
Ala Val Iso Leu Met Phe Tyr Trp Ser Thr Asn Gln Cys Pro Arg His Lys Asp Glu Orn Nle Nva Dab Hyp Ala Val Leu Met Phe Tyr Trp Ser Asn Gln Pro Arg His Lys Asp Glu Orn Nle
L amino acids
D amino acids

**Figure S4. Secondary plots of initial rate experiments.** Each error bar represents the standard deviation of four trials. Lines were fit using the equations described in the method section above. **A) PaNAS**. Initial reaction rates measured as NADPH was oxidized by PaODH. L-histidine concentration was varied from 0.78 µM to 200 µM. **B) SaNAS**. Initial reaction rates were measured as NADPH was oxidized by SaODH. D-histidine concentration was varied from 0.78 µM to 400 µM.

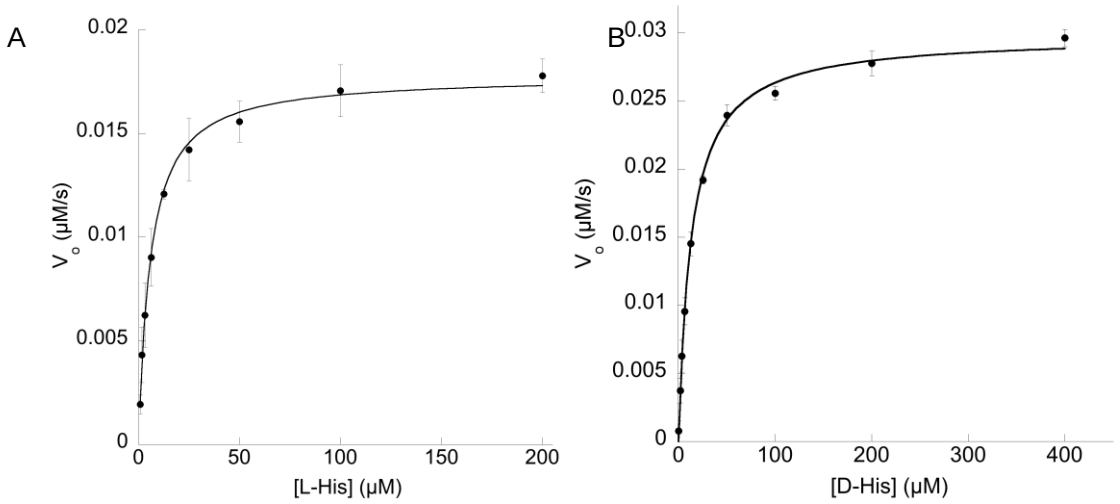


**Figure S5. Pseudopaline mass spectrometry data. A)** Extracted ion chromatogram for pseudopaline. The majority of pseudopaline eluted in the first peak at 0.33 min. **B)** ESI-MS spectrum for the 0.33 min elution peak showing pseudopaline. **C)** ESI-MS high resolution spectrum for pseudopaline from the 0.33 min elution peak. **D)** ESI-MS spectrum for the 1.51 min elution peak showing the NAS product. **E)** ESI-MS spectrum for pseudopaline following direct injection of supernatants.

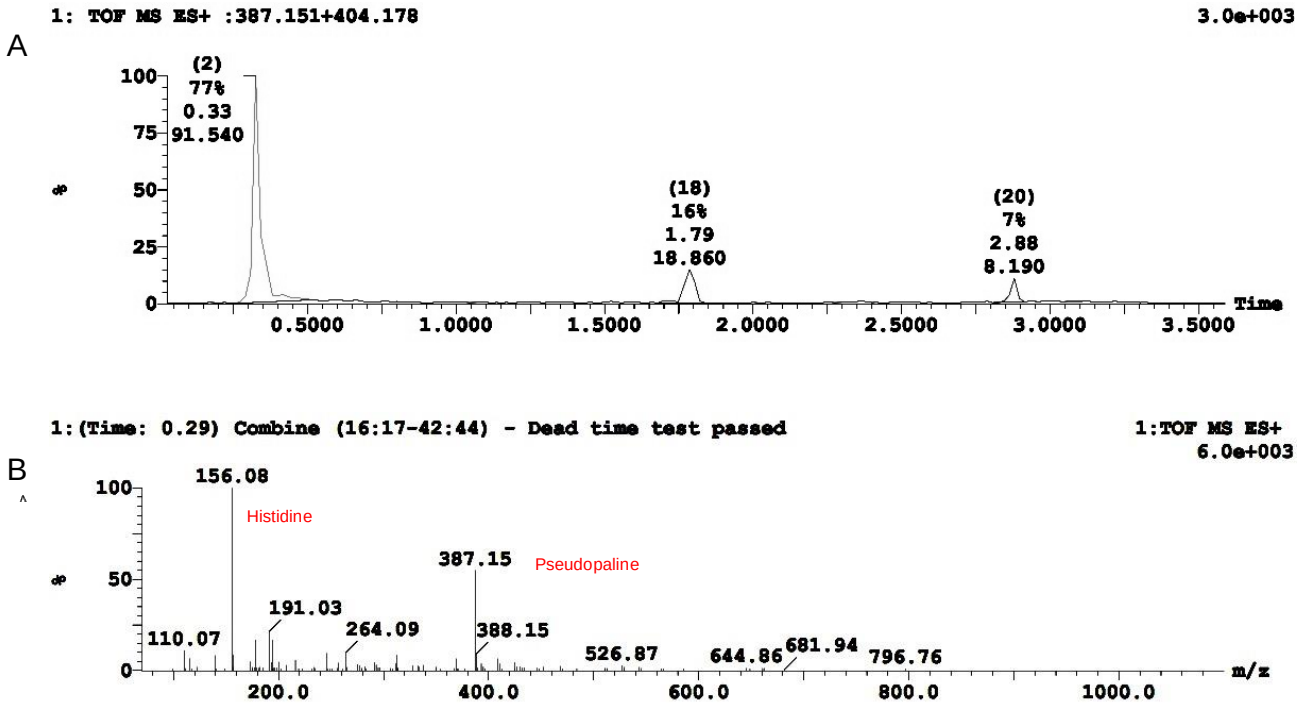

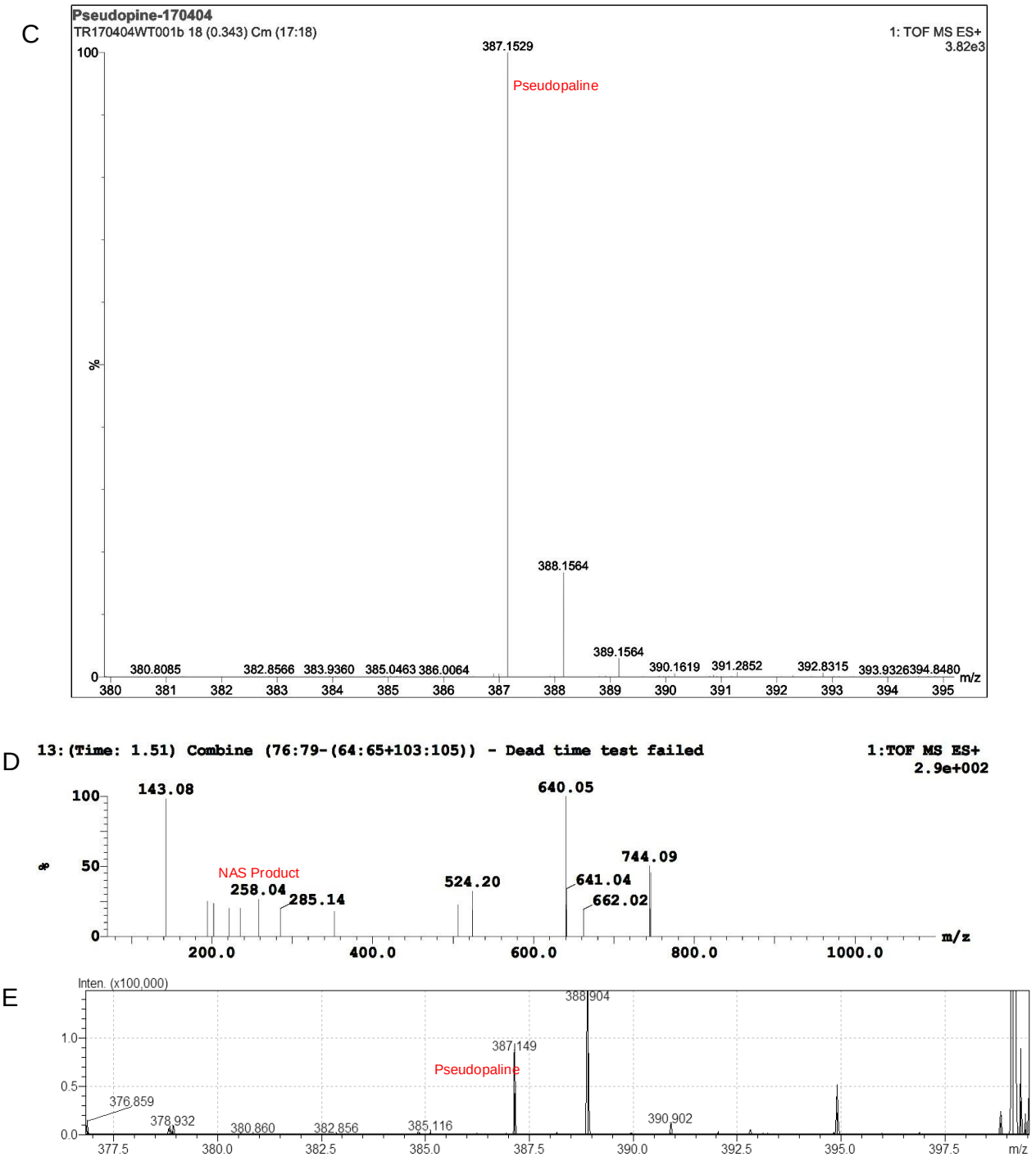


**Figure S6. Staphylopine mass spectrometry data. A)** Extracted ion chromatogram for staphylopine. The majority of staphylopine eluted in the first peak at 0.33 min. **B)** ESI-MS high resolution spectrum for staphylopine from the 0.33 min elution peak. **C)** ESI-MS spectrum for staphylopine following direct injection of supernatants.

A

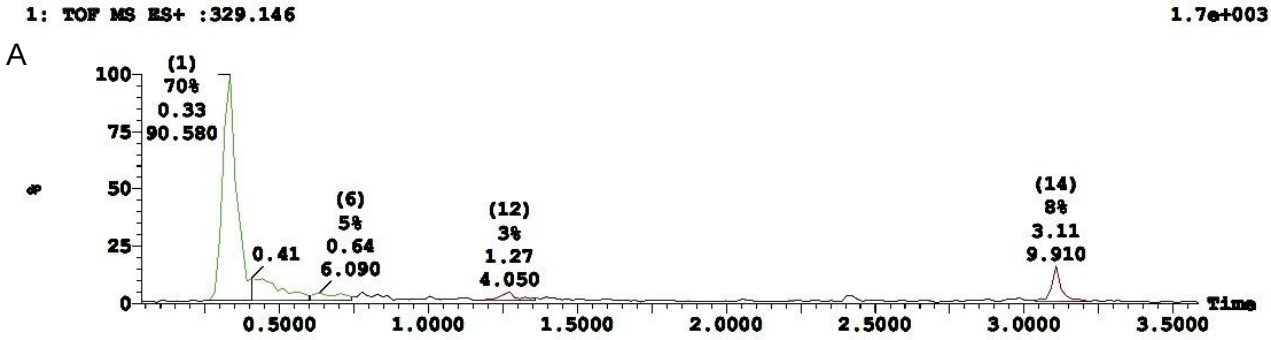
1: TOF MS ES+ :329.146
1.7e+003
(1)
70%
0.33
90.580
0.41
(6)
5%
0.64
6.090
(12)
3%
1.27
4.050
(14)
8%
3.11
9.910
Time

B

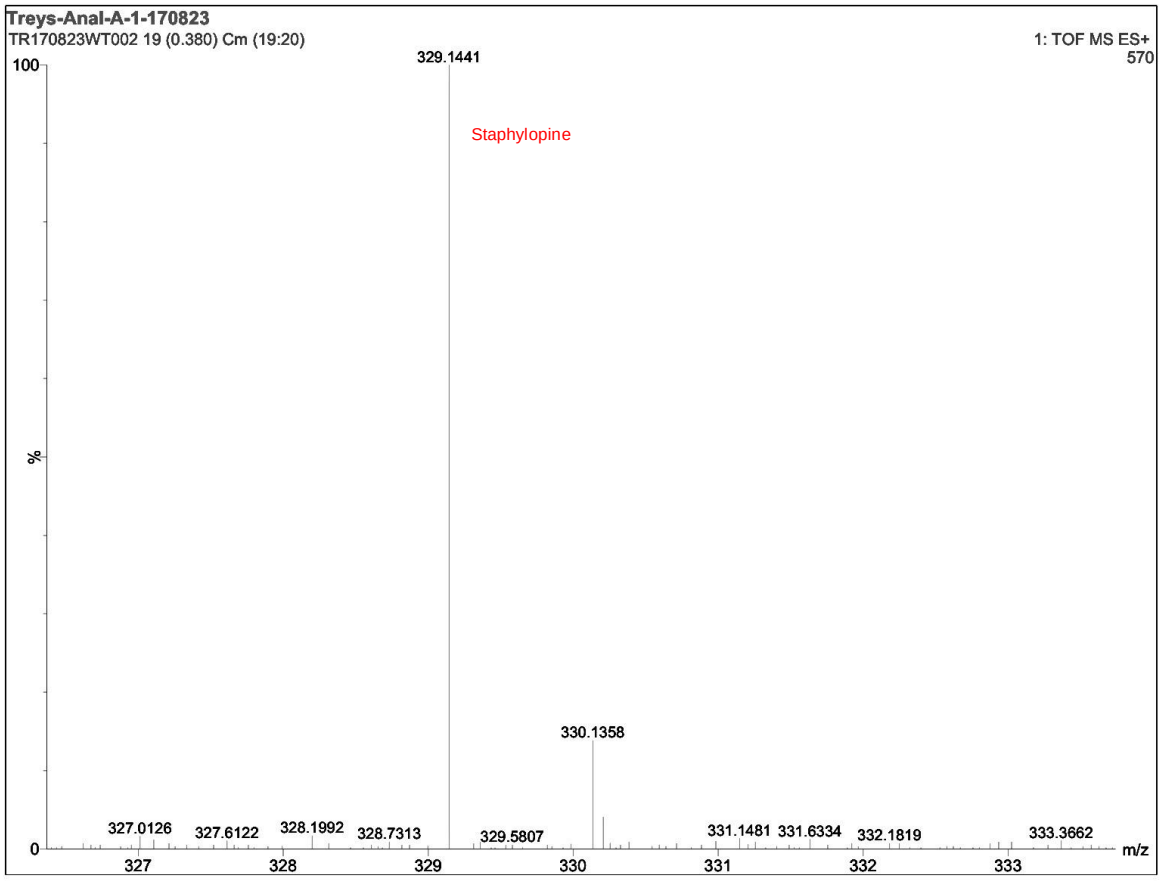
Treys-Anal-A-1-170823
TR170823WT002 19 (0.380) Cm (19:20)
1: TOF MS ES+
570
329.1441
Staphylopine
330.1358
327.0126
327.6122
328.1992
328.7313
329.5807
331.1481
331.6334
332.1819
333.3662
m/z

C

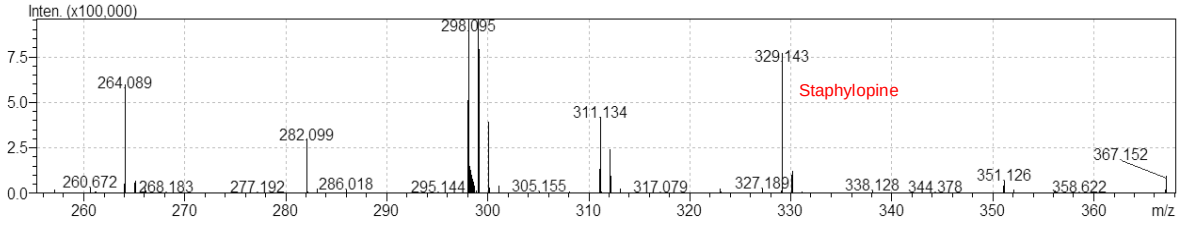
Inten. (x100,000)
298.095
329.143
Staphylopine
264.089
311.134
282.099
367.152
351.126
m/z

**Table S1. Compounds tested.**

| **L-Amino Acids** | **D-Amino Acids** |
|---|---|
| L-2,4-diaminobutyric acid | D-alanine |
| L-alanine | D-arginine |
| L-arginine | D-asparagine |
| L-asparagine | D-aspartic acid |
| L-aspartic Acid | D-glutamic acid |
| L-cysteine | D-glutamine |
| L-glutamic Acid | D-histidine |
| L-glutamine | D-leucine |
| L-histidine | D-lysine |
| L-hydroxy-Proline | D-methionine |
| L-isoleucine | D-norleucine |
| L-leucine | D-ornithine |
| L-lysine | D-phenylalanine |
| L-methionine | D-proline |
| L-norleucine | D-serine |
| L-norvaline | D-tryptophan |
| L-ornithine | D-tyrosine |
| L-phenylalanine | D-valine |
| L-proline | |
| L-serine | **2-Keto acids** |
| L-threonine | pyruvate |
| L-tryptophan | oxaloacetate |
| L-tyrosine | α-ketoglutarate |
| L-valine | |

## References


[1] Winsor, G. L., Griffiths, E. J., Lo, R., Dhillon, B. K., Shay, J. A., and Brinkman, F. S. (2016) Enhanced annotations and features for comparing thousands of Pseudomonas genomes in the Pseudomonas genome database, *Nucleic Acids Res 44*, D646-653.

[2] Maegley, K. A., Gonzalez, L., Smith, D. W., and Reich, N. O. (1992) Cofactor and DNA Interactions in *Eco*RI DNA Methyltransferase, *Journal of Biological Chemistry 267*, 6.

[3] Lakowicz, J. R. (2006) *Principles of Fluorescence Spectroscopy*, 3rd ed., Springer, New York.

[4] Buldain, G., Santos, C. d. l., and Frydman, B. (1985) Carbon-13 Nuclear Magnetic Resonance Spectra of the Hydrate, Keto and Enol forms of Oxalacetic Acid, *Magnetic Resonance in Chemistry 23*, 4.

[5] Morrison, J. F. (1969) Kinetics of the reversible inhibition of enzyme-catalyzed reactions by tight-binding inhibitors, *Biochim Biophys Acta 185*, 269-286.

[6] Ghssein, G., Brutesco, C., Ouerdane, L., Fojcik, C., Izaute, A., Wang, S. L., Hajjar, C., Lobinski, R., Lemaire, D., Richaud, P., Voulhoux, R., Espaillat, A., Cava, F., Pignol, D., Borezee-Durant, E., and Arnoux, P. (2016) Biosynthesis of a broad-spectrum nicotianamine-like metallophore in Staphylococcus aureus, *Science 352*, 1105-1109.